

Coherent tunneling and quantum coherence oscillations at the atomic level¹

Marius Grigorescu

The evolution of the quantum wave packet describing an atom trapped in the surface-tip junction of the scanning tunneling microscope is investigated by using the time-dependent Schrödinger equation, and a quasi-classical Hamiltonian approach. The estimates concern a Xe atom in a biased double-well junction potential. The exact treatment shows that quantum coherence oscillations of the metastable ground state may occur at particular resonant values of the bias voltage. The effect of decoherence by partial localization is studied within the quasi-classical frame.

PACS: 03.65.Bz,73.40.Gk,61.16.Di

¹Report FT-416-June 1996, Institute of Atomic Physics, Bucharest

1 Introduction

The phenomenology of the wave function collapse and decoherence is a subject of wide interest, ranging from the conceptual framework of quantum mechanics [1, 2] to the physics of the quantum logic circuits.

Dynamical loss of coherence produced by possible non-linear terms in the time-dependent Schrödinger equation (TDSE) could be observed by measurements on driven hyperfine transitions in $^9\text{Be}^+$ ions [3]. Such non-linear terms can appear by the coupling to the environment [4], but they could also be intrinsically built into the quantum mechanics, as it was proposed by Ghirardi, Rimini and Weber to explain the paradoxes of the measurement theory [5]. The mean-field of molecules or atomic nuclei provided by the Hartree-Fock approximation breaks spontaneously the translation symmetry, and is localized in the inertial frame defined by the center of mass (CM). The CM motion can be quantized, removing the spurious effects of the symmetry breaking, but when the size of the objects increases towards the macroscopic level, (the object becomes "environment" for its constituents), physical localization may occur [6, 7].

The interplay between quantum coherence and wave function collapse appears particularly striking in the computation models of the quantum computers [8]. Therefore, a most interesting issue is to study the coherence properties of the physical systems at atomic level. Recent experiments have proved the existence of a coherent component for the electron tunneling in quantum dots [9], while quantum localization was predicted for atoms moving in the periodic potential created by a phase-modulated standing light field [10].

The purpose of this work is to investigate the feasibility of experiments on localization and decoherence for the CM wave function of the individual atoms, using the scanning tunneling microscope (STM). Since the first experiments on reversible atom transfer [11], STM may be considered as the ideal instrument for manipulating atoms or molecules. The bistable operation mode of STM can be understood assuming that the diffusion barrier on the surface is high enough to prevent the escape of the particle from the junction region, and that the motion takes place along the outer normal to the surface plane in an asymmetric, one-dimensional, double-well potential (DWP) [12]. In a DWP, an observable effect which is very sensitive to decoherence is the tunneling of a wave-packet ψ_0 with the energy below barrier [13]. If ψ_0 is a

Gaussian localized initially in the metastable well, and the quantum coherence is preserved in time, then complete tunneling to the stable well appears only in very special resonance conditions, by quantum coherence oscillations (QCO) [14].

The coupling to the environment affects the superposition principle and the quantum coherence property, and in the case of a dissipative force linear in the CM velocity, the QCO between the two wells may either be damped [15], or completely suppressed [16]. However, decoherence could be produced also by dissipative terms which only suppress the spreading of the wave packet (e.g. the "squeezing" dissipation [4]). In the asymmetric DWP, such terms may change the tunneling mechanism from QCO between wave functions with different shapes, to coherent tunneling (i.e. after barrier crossing the wave function retains its initial shape [14]).

In Sect. 2 it is shown that for a Xe atom placed in the STM surface-tip junction, reversible tunneling by QCO resonances could be observed. The irreversible switching mode is discussed in Sect. 3, within a quasi-classical model. Conclusions are summarized in Sect. 4.

2 The atomic quantum coherence oscillations

An isomeric state ψ_0 of a quantum particle in an asymmetric DWP has a QCO resonance if it is a linear superposition of two quasi-degenerate eigenstates ψ_d, ψ_u of the Hamiltonian, with energies $E_d \approx E_u$, such that $\Delta = |E_u - E_d|$ is much smaller than the average level spacing. In this case the localization probability in the stable well, $\rho(t)$, oscillates according to the law $\rho(t) = [1 - \cos(\pi t/T_{max})]/2$, with $T_{max} = \hbar\pi/\Delta$. In most physical situations the resonance conditions are not fulfilled, but particularly interesting are the systems where the potential depends on a parameter which may be changed continuously until there is resonance². For STM this parameter can be the surface-tip bias voltage U .

The present estimates are based on the potential function given in ref. [12] for Xe atoms in a fixed surface-tip geometry. This potential consists in a DWP term produced by the binding interaction energy, $V_p(x)$, (Fig. 1, dashed line) and the dipole term, $V_d(x) = -U\mu_0\{[0.3 + 0.7(w+x)^4/L^4]^{-1} -$

²Resonances in a three-well potential of variable width are presented in the application 2349433, *Long distance quantum transfer*, available at <http://cipo.gc.ca>

$[0.3 + 0.7(w - x)^4/L^4]^{-1}\}/2w$, where $\mu_0 = 0.3$ D, ($1\text{D}=3.335\times 10^{-30}$ C·m), $w = 2.2$ Å, and $L = 1.56$ Å. The X-axis is chosen normal to the surface, with the origin at the barrier top of the term V_p . This term is taken as a fourth order polynomial, with the metastable minimum $V_0 = V_p(x_0) = -12.7$ meV at $x_0 = -0.7$ Å, near surface, the barrier top $V_b = V_p(x_b) = 0.45$ meV at $x_b = 0$, and the stable minimum $V_g = V_p(x_g) = -23.2$ meV at $x_g = 0.89$ Å, close to the tip. At small bias the total potential $V(x) = V_p(x) + V_d(x)$ remains a DWP, with the coordinates x_0, x_b, x_g of the extrema close to the values given above. For negative bias of the surface the barrier height $E_b = V_b - V_0$ decreases, and at $U \approx -1.2$ V the isomeric minimum disappears.

The CM wave function for the metastable ground state of a Xe atom localized initially near surface is well approximated by the Gaussian wave packet $\psi_0(x) = (c_0/\pi)^{1/4} e^{-c_0(x-x_0)^2/2}$, where $c_0 = M\omega_0/\hbar$, M is the Xe mass, and $\omega_0 = \sqrt{V''(x_0)}/M$ is the classical oscillation frequency at x_0 in the harmonic approximation.

If there are no decoherence factors, the wave function at the moment t is

$$\psi(x, t) = e^{-i\hat{H}t/\hbar}\psi_0(x) \quad , \quad \hat{H} = -\frac{\hbar^2}{2M}\frac{\partial^2}{\partial x^2} + V_p(x) + V_d(x) \quad , \quad (1)$$

and can be obtained by integrating the TDSE

$$i\hbar\frac{\partial\psi}{\partial t} = \hat{H}\psi \quad (2)$$

with $\psi(x, 0) = \psi_0(x)$ as initial condition.

The TDSE can be solved numerically in a spatial grid $\{x_k\}$, $k=1, N$, using the leap-frog method [17]. However, the computation becomes much faster if the discrete form of Eq. (2) is integrated as a Hamilton system of equations. Thus, if $u_k(t) \equiv \text{Re}(\psi(x_k, t))$ and $v_k(t) \equiv \text{Im}(\psi(x_k, t))$ denote the real, respectively the imaginary part of the wave function $\psi(x, t)$ at the grid point x_k , then Eq. (2) becomes

$$2\hbar\dot{u}_k = \frac{\partial\mathcal{H}}{\partial v_k} \quad , \quad 2\hbar\dot{v}_k = -\frac{\partial\mathcal{H}}{\partial u_k} \quad , \quad (3)$$

with

$$\mathcal{H} = \sum_{k=1}^N u_k(\hat{H}u)_k + v_k(\hat{H}v)_k \quad , \quad (4)$$

$$(\hat{H}y)_k = -\frac{\hbar^2}{2M\ell^2} \left[\frac{y_{k+3} + y_{k-3}}{90} - 3\frac{y_{k+2} + y_{k-2}}{20} + 3\frac{y_{k+1} + y_{k-1}}{2} - \frac{49}{18}y_k \right] + [V_p(x_k) + V_d(x_k)]y_k .$$

In the present application the Hamiltonian system of Eq. (3) was defined considering $N = 321$ spatial grid points equally spaced by $\ell = 0.01 \text{ \AA}$ within the interval $[x_{min}, x_{max}] = [-1.2 \text{ \AA}, 2 \text{ \AA}]$. For a fast integration can be used the D02BAF routine of the NAG library [18], with the time step $dt = 6.58 \times 10^{-2}$ ps. The localization probability in the stable well of $V(x)$ is $\rho(t) = \int_{x_b}^{x_{max}} \psi^*(x, t)\psi(x, t)dx$, and within the time interval $[0, 20 \text{ ps}]$ attains a maximum which is represented in Fig. 2(A) as a function of the bias voltage U . The peaks indicate the QCO resonances. The first appears at $U = -1.141 \text{ V}$ for the potential V represented in Fig. 1 by solid line. This resonance corresponds to $\rho(t)$ shown in Fig. 2(B), with the maximum at the moment $T_{max} = 14.37 \text{ ps}$. In Fig. 1 can be seen the wave function at $t = 0$, (ψ_0 , dotted line), and at $t = T_{max}$, (ψ_M , solid line).

3 The coherent tunneling

During QCO the wave-packet changes its shape, and therefore the tunneling is not coherent. The issue of coherent tunneling may receive an answer from the study of the evolution pattern for wave functions constrained to be Gaussian all the time, as in the quantum molecular dynamics [19]. The constrained dynamics will be obtained by a time-dependent variational calculation within the trial manifold of the Gaussian wave packets with variable centroid and width. This manifold contains the isomeric ground state, and is represented by a combination between coherent and squeezed states,

$$\psi_c(z, s) = e^{(zb^\dagger - z^*b)} e^{(sb^\dagger b^\dagger - s^*bb)/2} \psi_0 , \quad z = \alpha + i\beta, \quad s = \rho e^{-2i\phi} , \quad (5)$$

with $(\alpha, \beta, \rho, \phi)$ real parameters, and $b = \sqrt{M\omega_0/2\hbar}(x - x_0 + \hbar\partial_x/M\omega_0)$ the Dirac-Fock annihilation operator for ψ_0 . In terms of the variables $x_c = x_0 + \alpha\sqrt{2\hbar/M\omega_0}$, $p_c = \beta\sqrt{2\hbar M\omega_0}$, $v = (\sinh \rho)^2$, the equations of motion obtained from the variational equation $\delta \int dt \langle \psi_c | i\hbar\partial_t - \hat{H} | \psi_c \rangle = 0$ are

$$\dot{x}_c = \frac{\partial \langle \psi_c | \hat{H} | \psi_c \rangle}{\partial p_c} \quad \dot{p}_c = -\frac{\partial \langle \psi_c | \hat{H} | \psi_c \rangle}{\partial x_c} , \quad (6)$$

$$\hbar\dot{\phi} = \frac{\partial\langle\psi_c|\hat{H}|\psi_c\rangle}{\partial v} \quad \hbar\dot{v} = -\frac{\partial\langle\psi_c|\hat{H}|\psi_c\rangle}{\partial\phi} . \quad (7)$$

Eqs. (6) describe the motion of the CM coordinate and momentum x_c, p_c of the Xe atom, while Eqs. (7) provide the evolution of the localization width around x_c , $\sigma_x^2 \equiv \langle\hat{K}\rangle = \langle x^2 \rangle - \langle x \rangle^2 = [1/2 + v + \sqrt{v(v+1)} \cos 2\phi]/c_0$. To express the average $\langle\psi_c|\hat{H}|\psi_c\rangle$ in analytical form, the potential $V(x)$ was replaced by a fourth order interpolation polynomial, $V_{pol}(x)$, with coefficients determined by fit.

At the first resonance ($U = -1.141$ V), the best fit of the potential $V(x)$ (Fig. 1, solid line) is given by a quartic polynomial $V_{pol}(x)$ (Fig. 3(A), solid line), with the extremum values of 0.8 meV, 1.85 meV and -48.88 meV at the points $x_0 = -0.47$ Å, $x_b = -0.19$ Å, and $x_g = 1.01$ Å, respectively. The classical oscillation frequency at x_0 which defines ψ_0 in Eq. (5) is $\omega_0 = 1.95$ ps $^{-1}$. Using these results, \hat{H} at resonance is well approximated by $\hat{H}_{pol} = -\hbar^2\partial_x^2/2M + V_{pol}(x)$, and $V_{av}(x) \equiv \langle\hat{H}_{pol}\rangle(x_c = x, p_c = 0, v, \phi)$ has the role of effective potential for the CM dynamics of the Gaussian wave packet ψ_c . This function is represented for $\phi = 0$ and $v = 0, 0.1, 0.5, 1, 1.5, 2$ in Fig. 3(A) by dashed lines. If $v = 0$, then $V_{av}(x)$ is also a DWP, with the extremum values of 1.57 meV, 1.97 meV and -46.8 meV at -0.425 Å, -0.215 Å, and 1 Å, respectively. Thus, for a Gaussian wave packet the effective potential is not the same as for the classical particle, and the top of the barrier has a small shift to higher energy.

When $x_c = x_0$ and $p_c = v = \phi = 0$, the trial function ψ_c reduces to the isomeric ground state ψ_0 of \hat{H}_{pol} . The quasi-classical dynamics of a Xe atom which is initially in this state was obtained by integrating the system of Eqs. (6),(7) using the routine D02BAF of the NAG library, and the trajectory $x_c(t)$ is represented in Fig. 3(B) by dashed line. For comparison, the exact wave function $\psi(t) = \exp(-it\hat{H}_{pol}/\hbar)\psi_0$ was calculated by solving the TDSE, and the corresponding expectation value $x_{QCO}(t) = \langle\psi(t)|x|\psi(t)\rangle$ is represented in Fig. 3(B) by solid line. Initially $x_c(t)$ and $x_{QCO}(t)$ are close, but in time $x_{QCO}(t)$ extends across the barrier, while $x_c(t)$ oscillates in the isomeric well with small amplitude³.

³Numerical estimates indicate that if the "squeezing" dissipation term provided by the coupling operator $\hat{K} = (x - \langle\psi|x|\psi\rangle)^2$ is included, and $\psi(t)$ is obtained by integrating the non-linear TDSE $i\hbar\partial_t\psi = (\hat{H}_{pol} + \kappa\hat{K}\partial_t\langle\psi|\hat{K}|\psi\rangle)\psi$, then for $\kappa \sim 50\hbar/\text{Å}^4$ any significant changes in the shape of ψ are suppressed, and $\langle\psi(t)|x|\psi(t)\rangle$ remains close to $x_c(t)$.

The oscillation amplitude of x_c increases with the energy $E_c = \langle \psi_c | \hat{H}_{pol} | \psi_c \rangle$, but the trajectory remains confined in the isomeric well until E_c reaches a narrow interval very close to the barrier top of V_{av} , when a "switching" mode appears. For an orbit with the initial conditions $x_c \sim -0.25 \text{ \AA}$, $p_c = v = \phi = 0$, the oscillations in the isomeric well are interrupted by a sudden jump to the stable well, where the particle keeps oscillating without return. This interesting behaviour resembles the experimental situation, because the observed atom switching occurs with a rate proportional to a power of the current, and could be explained by the electron heating effects [11, 12]. Here, this mode is due to a small valley connecting the two wells which appears near the barrier top of V_{av} in the squeezing dimension. Thus, the escape to the stable well becomes possible when the four dimensional orbit $\mathcal{C}_t \equiv (x_c, p_c, v, \phi)(t)$ is directed along this valley. The projection of the switching mode orbit \mathcal{C} on the CM phase space plane is pictured in Fig. 4(A), while the corresponding trajectory plot, $x_c(t)$, is shown in Fig. 4(B).

4 Conclusions

The TDSE calculations indicate that if quantum coherence is preserved, then elastic tunneling of the Xe atom can appear only at certain resonant values of the bias voltage. At resonance the atom oscillates between a localized state on the surface (ψ_0), and a state close to tip (ψ_M), with a frequency attaining the maximum ($\sim 1/2T_{max} = 34.8 \text{ GHz}$) at the first resonance ($U \sim -1.141 \text{ V}$). Thus, the exact treatment of the atom tunneling in the STM potential predicts an oscillatory behavior which cannot explain the irreversible switching mode. The observation of irreversible transfer with a constant rate indicates that in the present experiments the phase coherence is destroyed by the voltage pulse, or by other external factors, like dissipation. According to the quasi-classical results, the switching might be explained by a decoherence mechanism producing excitation and partial localization.

The atomic QCO in STM might be observed as oscillations of the junction impedance, which changes when the atom moves from surface to the tip [11]. Therefore, accurate measurements of the resonant bias voltages and of the transfer time-scale could provide significant insight on the mechanism of decoherence and localization at the atomic level.

References

- [1] M. Gell-Mann and J. B. Hartle, Phys. Rev. **D 47**, 3345 (1993).
- [2] W. H. Zurek, Phys. Rev. **D 24**, 1516 (1981), **D 26**, 1862 (1982).
- [3] S. Weinberg, Phys. Rev. Lett. **62**, 485 (1989).
- [4] M. Grigorescu and N. Cârjan, Phys. Rev. E **51**, 1996 (1995).
- [5] G. C. Ghirardi, A. Rimini and T. Weber, Phys. Rev. D **34**, 470 (1986).
- [6] D. Vitali, L. Tessieri and P. Grigolini, Phys. Rev. A **50**, 967 (1994).
- [7] L. Tessieri, D. Vitali and P. Grigolini, Phys. Rev. A **51**, 4404 (1995).
- [8] P. W. Shor, Phys. Rev. **A 52**, R2493 (1995).
- [9] A. Yacoby, M. Heiblum, D. Mahalu and H. Shtrikman, Phys. Rev. Lett. **74**, 4047 (1995).
- [10] P. J. Bardroff, I. Bialynicki-Birula, D. S. Hrähmer, G. Kurizki, E. Mayr, P. Stifter and W. P. Schleich, Phys. Rev. Lett. **74**, 3959 (1995).
- [11] D. M. Eigler, C. P. Lutz and W. E. Rudge, Nature **352**, 600 (1991).
- [12] R. E. Walkup, D. M. Newns and Ph. Avouris, Phys. Rev. B **48**, 1858 (1993).
- [13] A. J. Leggett, in *Proc. 4th Int. Symp. Foundations of Quantum Mechanics*, Tokyo, 1992, JJAP Series 9 (1993), p.10.
- [14] M. M. Nieto, V. P. Gutschick, C. M. Bender, F. Cooper and D. Strottman, Phys. Lett. **163 B**, 336 (1988).
- [15] V. A. Benderskii, V. I. Goldanskii and D. E. Makarov, Phys. Rep. **233**, 195 (1993).
- [16] A. J. Bray and M. A. Moore, Phys. Rev. Lett. **49**, 1545 (1982).
- [17] J. M. Hyman, *Advances in Computer Methods for Partial Differential Equations-III*, edited by R. Vichevetski and R. S. Stepleman (IMACS, Bethlehem, PA, 1979), p. 313.

[18] *The NAG Fortran Library Manual, Mark 15*, 1st Edition, June (1991).

[19] J. Aichelin, Phys. Rep. **202**, 233 (1991).

Figure Captions

Fig. 1. The potential V at $U = -1.141$ V (solid), $U = 0$ (dash), and the wave functions ψ_0 , ψ_M (in units of $\text{\AA}^{-1/2}$) as a function of distance.

Fig. 2. The maximum value attained by ρ within 20 ps as a function of the bias voltage (A) and ρ as a function of time at the first resonance (B).

Fig. 3. The polynomial potential V_{pol} (solid) and the average potential V_{av} (dash) for $v = 0, 0.1, 0.5, 1, 1.5, 2$, as a function of distance (A); x_{QCO} (solid) and x_c (dash) as a function of time (B).

Fig. 4. The switching mode: phase-space orbit of the CM motion (A) and the CM coordinate as a function of time (B).

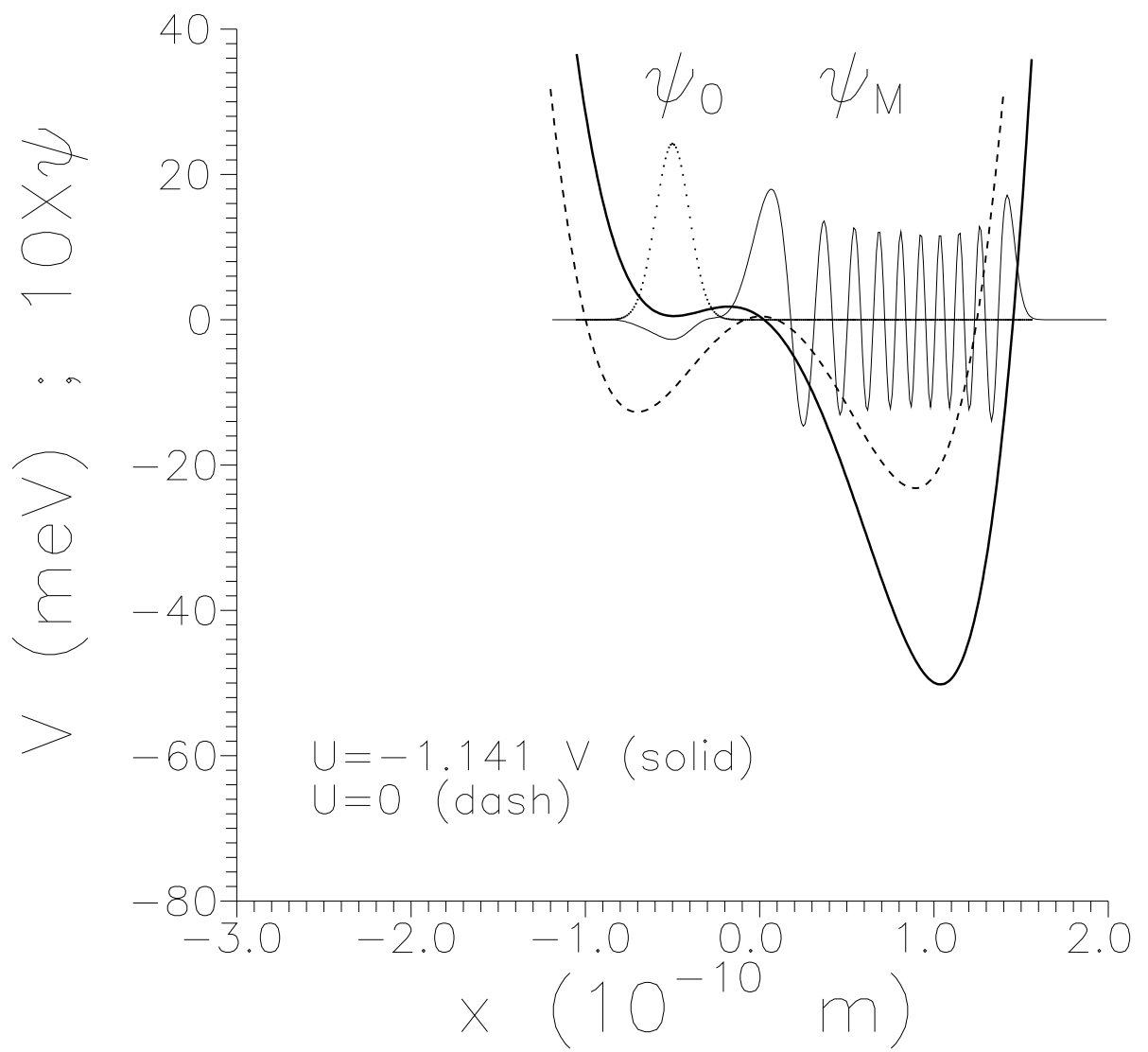


Fig. 1

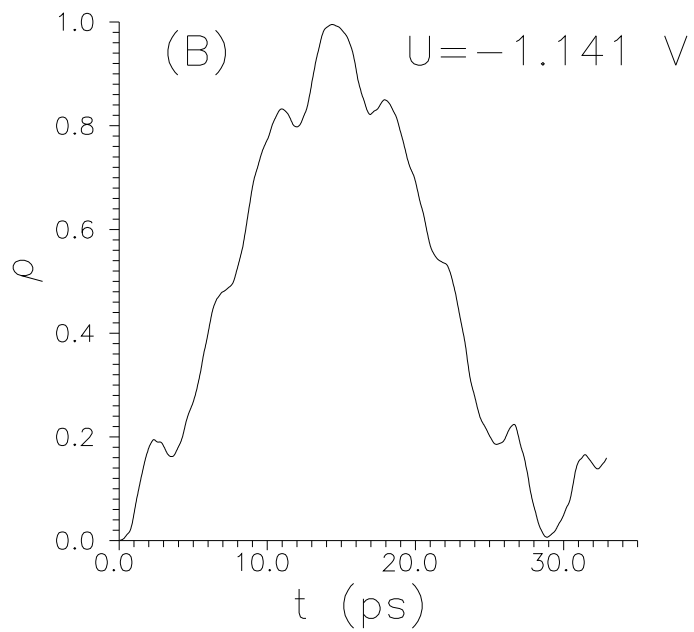
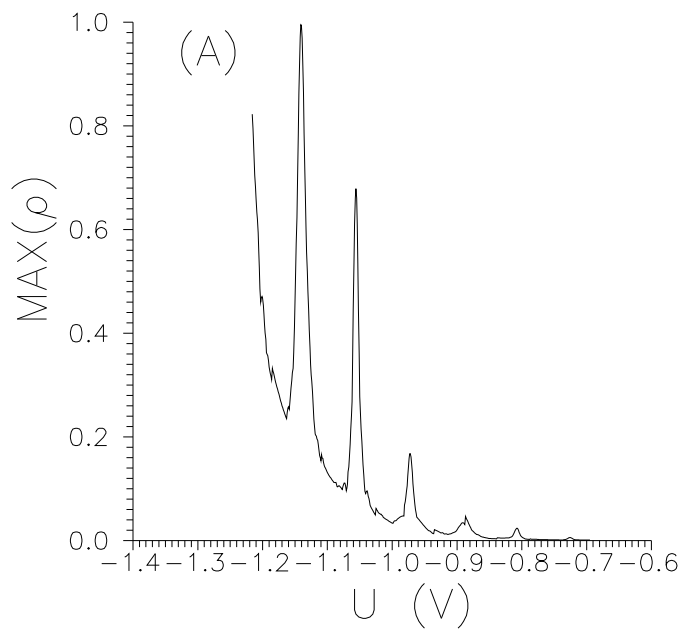


Fig. 2

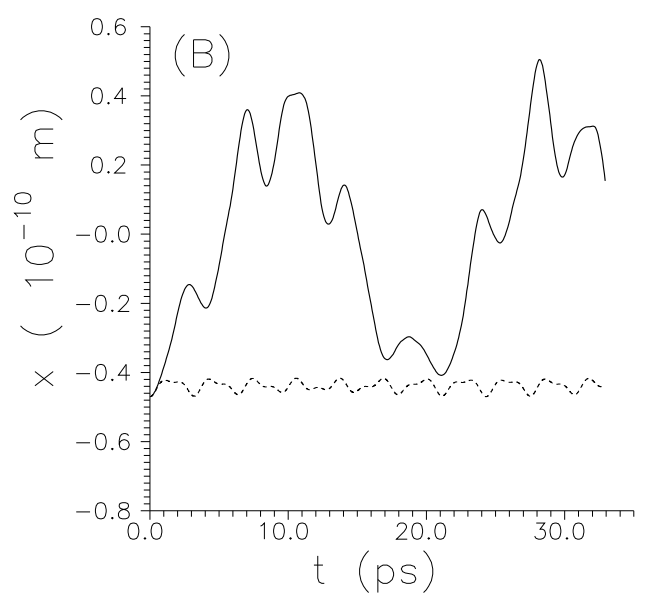
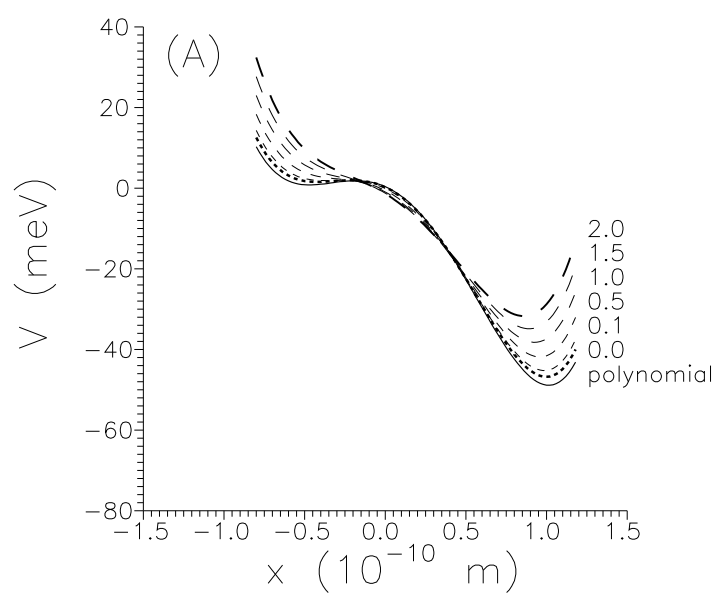


Fig. 3

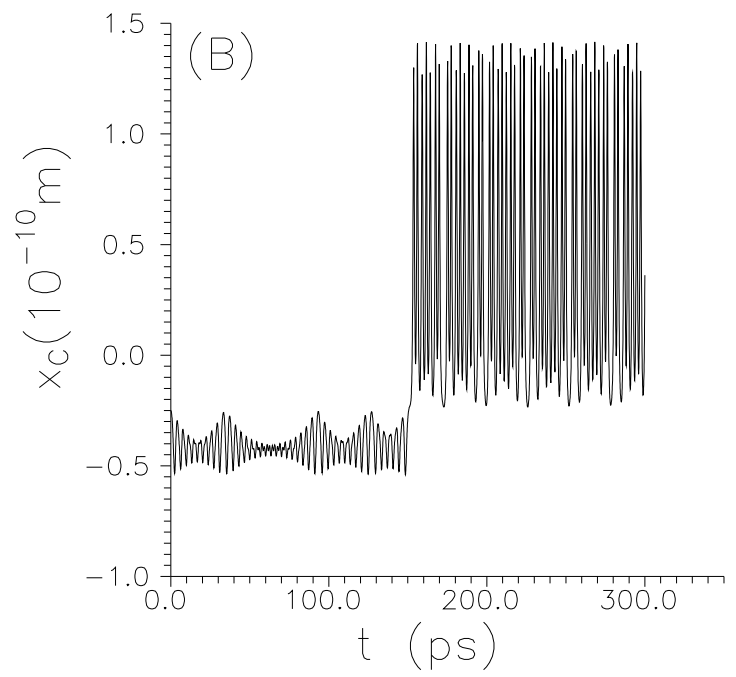
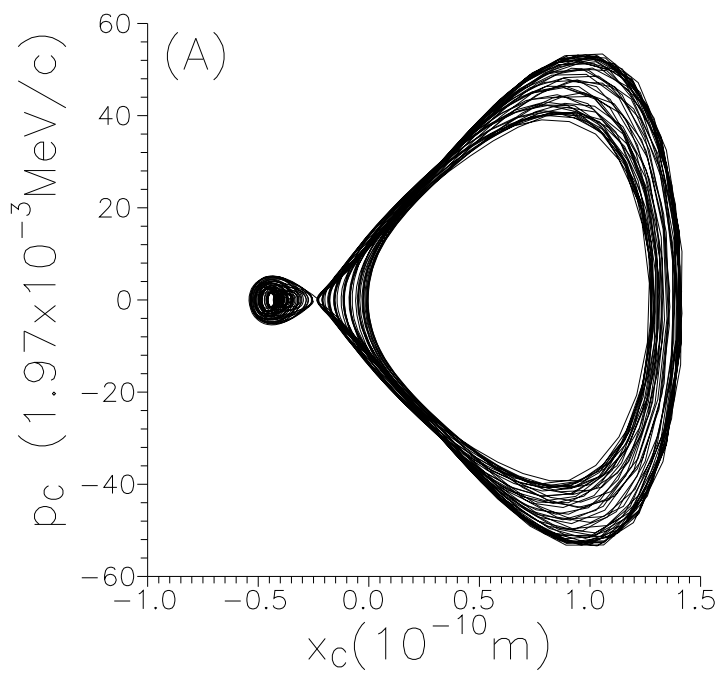


Fig. 4